

MOL #26690

**AMPHETAMINE INDUCES A CAMKII-DEPENDENT REDUCTION IN  
NOREPINEPHRINE TRANSPORTER SURFACE EXPRESSION LINKED TO CHANGES  
IN SYNTAXIN 1A/TRANSPORTER COMPLEXES**

Concetta Dipace, Uhna Sung, Francesca Binda, Randy D. Blakely and Aurelio Galli

Department of Molecular Physiology and Biophysics (C.D., F.B., A.G.)

Center for Molecular Neuroscience (C.D., U.S., F.B., RD.B., A.G.)

Department of Pharmacology (U.S., RD. B.)

Vanderbilt University

465 21<sup>st</sup> Ave. South

Nashville, TN 37232-8548

MOL #26690

## Running Title Page

1. Running title: Amphetamine-Mediated NET Trafficking

2. Corresponding author:

Aurelio Galli, Ph.D.

Department of Molecular Physiology and Biophysics

Center for Molecular Neuroscience

Vanderbilt University Medical Center

465 21st Avenue South

7124A Medical Research Building III

Nashville, TN 37232

Tel: 615-936-3891

Fax: 615-936-3745

E-mail: aurelio.galli@vanderbilt.edu

3. Number of text pages: 28

Number of tables: N/A

Number of figures: 6

Number of references: 44

Number of words in the abstract: 225

Number of words in the introduction: 1014

Number of words in the discussion: 1287

4. List of nonstandard abbreviations used in the paper:

AMPH, amphetamine; NE, norepinephrine; NET, norepinephrine transporter; CaMKII, calcium/calmodulin-dependent protein kinase II; SYN1A, syntaxin 1A;

MOL #26690

## ABSTRACT

Norepinephrine (NE) transporters (NETs) are high-affinity transport proteins that mediate the synaptic clearance of NE following vesicular release. NETs represent a major therapeutic target for antidepressants and are also targets of multiple psychostimulants including amphetamine (AMPH) and cocaine. Recently, we demonstrated that syntaxin 1A (SYN1A) regulates NET surface expression and, through binding to the transporter's NH<sub>2</sub> terminus, regulates transporter catalytic function. AMPH induces NE efflux and may also regulate transporter trafficking. We monitored NET distribution and function in catecholaminergic cell lines (CAD) stably transfected with either full-length human NET (CAD-hNET) or with an hNET N-terminal deletion (CAD-hNET $\Delta_{28-47}$  cells). In hNET-CAD cells, AMPH causes a slow and small reduction of surface hNET with a modest increase in hNET/SYN1A associations at the plasma membrane. In contrast, in CAD-hNET $\Delta_{28-47}$  cells, AMPH induces a rapid and substantial reduction in surface hNET $\Delta_{28-47}$  accompanied by a large increase in plasma membrane hNET $\Delta_{28-47}$ /SYN1A complexes. We also found that AMPH in CAD-hNET $\Delta_{28-47}$  cells induces a robust increase in cytosolic Ca<sup>2+</sup> and concomitant activation of calcium/calmodulin-dependent protein kinase II (CaMKII). Inhibition of either the increase in intracellular Ca<sup>2+</sup> or CaMKII activity blocks AMPH stimulated hNET $\Delta_{28-47}$  trafficking as well as the formation of hNET $\Delta_{28-47}$ /SYN1A complexes. Here, we demonstrate that AMPH stimulation of CaMKII stabilizes a hNET/SYN1A complex. This hNET/SYN1A complex rapidly redistributes, upon AMPH treatment, when mechanisms supported by the transporter's NH<sub>2</sub> terminus are eliminated.

MOL #26690

## INTRODUCTION

NET is responsible for the presynaptic elimination of NE following release at noradrenergic synapses (Iversen, 1971; Trendelenburg, 1991). NETs are targets for various psychostimulants, including cocaine and amphetamine (AMPH), and are antagonized by multiple antidepressants (Tatsumi et al., 1997). Topological predictions indicate that NET and its homologs bear 12 transmembrane domains (TMD) with intracellular NH<sub>2</sub> and COOH termini. The 12 TMD topology has recently been supported by the high resolution structure of LeuT, a prokaryotic sodium-dependent leucine transporter with significant homology to NET and related neurotransmitter transporters (Yamashita et al., 2005).

The intracellular domains of NET have numerous putative phosphorylation sites for various protein kinases, and multiple protein kinases have been suggested to regulate NET function (Blakely et al., 2005). For example, muscarinic receptors (e.g. M<sub>3</sub>) that are able to stimulate phospholipase C and protein kinase C (PKC), can induce the loss of cell surface NETs with a consequent loss of transport activity (Apparsundaram et al., 1998). Consistent with this observation, phorbol esters trigger a loss of NET surface expression in heterologous expression systems, rat vas deferens as well as in forebrain synaptosomes (Apparsundaram et al., 1998; Sung et al., 2003) and NETs, like the serotonin transporter (SERT) and dopamine transporter (DAT) proteins, become phosphorylated (Cervinski et al., 2005; Jayanthi et al., 2004). Still, the mechanisms activated by transporter phosphorylation have not been clarified. Additionally, several hormones and signaling pathways can positively regulate NET function, including angiotensin (Lu et al., 1998; Lu et al., 1996; Yang and Raizada, 1998) and insulin (Apparsundaram et al., 2001).

Recently, attention has been drawn to the physical and functional interactions of NET and related transporters with the t-SNARE protein, SYN1A (Deken et al., 2000; Quick, 2003; Sung et al., 2003; Wang et al., 2003). These studies suggest that in addition to its classical role of supporting vesicular fusion, SYN1A also controls neurotransmission by regulating both plasma membrane trafficking and transporter function. (Beckman and Quick, 1998; Blakely and Sung,

MOL #26690

2000; Gonzalez and Robinson, 2004; Sung et al., 2003). With regard to NET, we have shown that a) NET colocalizes and forms stable complexes with SYN1A; b) NET/SYN 1A interactions are direct, mediated by the cytoplasmic domain of SYN1A and the NH2 terminus of NET; and c) stimuli known to trigger NET redistribution, such as PKC activation, modulate NET/SYN1A interactions (Sung et al., 2003). Sung and collaborators demonstrated that deletion of the first 42 amino acids of hNET (hNET $\Delta_{2-42}$ ) abolishes the NET/SYN1A interaction. However, as we demonstrate below, smaller mutations such as hNET $\Delta_{28-47}$  can preserve and/or enhance this interaction, and become useful tools for studying the coordination of hNET regulation by associated proteins.

AMPH, like NE, serves as a substrate for NET (Wall et al., 1995) and also promotes transport reversal, triggering vesicle-independent NE release (Burnette et al., 1996; Pifl and Singer, 1999; Wall et al., 1995). AMPH also influences biogenic amine transporters trafficking, best studied with the homologous DAT (Gonzalez and Robinson, 2004; Johnson et al., 2005; Kahlig and Galli, 2003; Saunders et al., 2000). Fleckenstein and colleagues demonstrated that a single systemic injection of AMPH (Fleckenstein et al., 1999) induces a significant attenuation in DA uptake into striatal synaptosomes when prepared within one hour after administration, effects that are reversible and appear to arise from a decrease in DAT  $V_{max}$ , suggesting that the number of DAT proteins on the plasma membrane can be downregulated by acute AMPH exposure. Similarly, Gulley has shown that AMPH exposure to DAT-expressing oocytes (Gulley et al., 2002) or to native DAT expressed in the nucleus accumbens (Gulley et al., 2002) diminishes DAT-mediated currents and DA clearance, respectively. Still, it has to be determined whether similar AMPH actions apply to NET. Also, it is unclear how psychostimulant-modulated transporter trafficking links to the emerging biology of transporter-associated proteins, such as SYN1A.

In the current report, we demonstrate that AMPH-induced hNET trafficking away from the plasma membrane, a response negatively modulated by the transporter's NH2 terminus, as inferred from the properties of a deletion, hNET $\Delta_{28-47}$ , that demonstrates more rapid and extensive AMPH-induced transporter redistribution. We propose that normally, this regulation suppresses AMPH-

MOL #26690

induced increase in intracellular  $\text{Ca}^{2+}$  and possibly CaMKII-dependent modulatory pathways that lead, among other things, to changes in NET surface expression and formation of NET/SYN1A associations. However, such protective mechanisms also afford an opportunity for genetic or environmental modulation to disinhibit this process and greatly enhance AMPH action. We discuss our findings in terms of models of AMPH sensitization linked to  $\text{Ca}^{2+}$ /CaMKII-dependent changes in monoamine signaling.

## MATERIALS AND METHODS

**Cell culture and transfection.** CAD cells (Qi et al., 1997) are catecholaminergic cells that express SYN1A (Sung et al., 2003) and provide an appropriate parental background for studying hNET trafficking because of their lack of NET expression, inability to uptake [ $^3\text{H}$ ]NE (Sung et al., 2003), and their lack of desipramine- (DS) and cocaine-sensitive whole-cell currents (Binda et al., 2005). CAD cells were maintained in DMEM/F-12 medium supplemented with 8% fetal bovine serum (FBS), 2 mM L-glutamine (L-Glu), 100 IU/ml penicillin, and 100  $\mu\text{g}/\text{ml}$  streptomycin (pen/strep) in a humidified incubator at  $37^\circ\text{C}$  and 5%  $\text{CO}_2$ . The hNET (Pacholczyk et al., 1991) and HA-hNET $\Delta_{28-47}$  (this report) were cloned into pcDNA3, and stably transfected into CAD cells using Lipofectin (Invitrogen, San Diego, CA), and selected and maintained in 200  $\mu\text{g}/\text{ml}$  of G418 (Mediatech, Herndon, VA). hNET $\Delta_{28-47}$  is a hNET variant recovered during the course of expression experiments seeking to evaluate requirements for SYN1A modulation of hNET and unlike hNET $\Delta_{2-42}$  (Sung et al., 2003), supports efficient SYN1A interactions. The deletion mutant hNET $\Delta_{28-47}$  was generated by oligonucleotide site directed mutagenesis using Quick change mutagenesis kit (Stratagene, La Jolla, CA) (Sung et al., 2003). Initial studies examining AMPH effects demonstrated a more robust trafficking response with this mutant as compared to hNET, and thus we incorporated this mutant into our ongoing studies of hNET regulation. Transient transfections were performed with Eugene 6 (Roche, Indianapolis, IN). Typically, 1  $\mu\text{g}$  cDNA was

MOL #26690

transfected into 500,000 cells in each well of a six-well plate. Cells were transfected 48 hr prior to transport or biochemical assays.

**Antibodies and other reagents.** Anti-hemagglutinin (HA) antibody (3F10) (Boehringer Mannheim, Mannheim, Germany) and monoclonal NET17-1 (Mab technologies, Atlanta) were used at a dilution of 1:500 and 1:1000, respectively, for immunoblots and identification of NET proteins by ECL reaction. Anti-hemagglutinin (HA) rat monoclonal antibody (3F10) (Boehringer Mannheim) and monoclonal anti-histidine (anti-His) antibody (Clontech, Palo Alto, CA) were used (1  $\mu$ g) for immunoprecipitation of hNET $\Delta_{28-47}$  and hNET, respectively. Immunoblots for SYN1A were performed by using anti-HPC-1 antibody (Sigma, St.Louis, MO) at a dilution of 1:2000. In addition, immunoblots of total and phosphorylated CaMKII were performed using anti-CaMKII (Cell Signaling Technology, Danvers, MA) (1:1000) and anti-phospho-CaMKII (Abcam, Cambridge, MA) (1:2000), respectively. Microcystin-LR was obtained from Alexis (San Diego, CA); BAPTA-AM and Oregon Green BAPTA-AM were purchased from Molecular Probes (Eugene, OR); KN-93 and KN-92 were obtained from Calbiochem (San Diego, CA); AMPH and desipramine were acquired from Sigma.

**Cell surface biotinylation.** Biotinylation experiments were performed on intact cells to evaluate changes of hNET and hNET $\Delta_{28-47}$  cell surface expression as previously described (Garcia et al., 2005; Saunders et al., 2000; Sung et al., 2003). Briefly, 48 hr before each experiment, cells were plated at a density of  $1 \times 10^6$  per well in a 6-well poly-d-lysine (Sigma) coated plate. After each treatment, cells were washed with PBS containing  $\text{Ca}^{2+}/\text{Mg}^{2+}$ , and incubated with 1.0 mg/ml sulfosuccinimidyl-2-(biotinamido)ethyl-1,3-dithiopropionate-(sulfo-NHS-SS-biotin, Pierce, Rockford, IL) for 30 min at 4°C, washed, quenched with 100 mM glycine, extracted in lysis buffer (PBS  $\text{Ca}^{2+}/\text{Mg}^{2+}$ , 1% Triton 100-X, 0.5 mM PMSF), and incubated with Immunopure immobilized Streptavidin beads (Pierce) for 1hr at room temperature. Beads were washed 3 times in lysis buffer,

MOL #26690

and proteins bound to Streptavidin beads were eluted in 2X Laemmli buffer containing 2-mercaptoethanol (Laemmli, 1970). Samples were then analyzed by SDS-PAGE (7.5% gel) and immunoblotted as described for Western blot analyses. For estimation of relative amounts of proteins, the exposed films of the immunoblots were scanned and the captured images were processed and quantitated with SCION Image (Scion Corporation).

**Co-Immunoprecipitations.** To examine changes in hNET $\Delta_{28-47}$  and hNET/SYN1A interactions, co-immunoprecipitation experiments were performed. CAD cells transiently transfected either with His-hNET or HA-hNET $\Delta_{28-47}$  and SYN1A were plated at a density of  $1 \times 10^5$  per well in 6 well poly-d-lysine (Sigma) coated plates. After each treatment, cells were washed with cold PBS/ $\text{Ca}^{2+}$ / $\text{Mg}^{2+}$  and incubated in 400  $\mu\text{l}$ /well of lysis buffer [containing (in mM) 50  $\text{NaH}_2\text{PO}_4$ , 10 Tris, 100 NaCl, 0.5 PMSF, pH 8.0, plus 1% Triton X-100] for 1 hr at 4°C. Cell lysates recovered by centrifugation at  $20,000 \times g$  for 30 min were incubated overnight at 4°C either with anti-His or with anti-HA (3F10) antibodies. Complexes were retrieved by the addition of 20  $\mu\text{l}$  of protein G-Sepharose (Amersham Biosciences) and washed 3 times with lysis buffer. For the coimmunoprecipitation of surface complexes (hNET/SYN1A), cells were biotinylated with EZ-link NHS-sulfo-S-S-biotin (Pierce) and lysed as described above. Monomeric avidin beads (40  $\mu\text{l}$  of beads (Pierce)/one well cell lysate) were preblocked with 10 mg/ml BSA (30 min at 4 °C) and then used to obtain biotinylated proteins. Then, avidin beads were washed 5 times at room temperature with lysis buffer and the bound proteins were eluted with lysis buffer containing 4 mM biotin (Sigma). Anti-His or anti-HA antibodies were added to the eluted proteins, processed for immunoprecipitation and analyzed as described above. Multiple films were exposed for each immunoblot to insure linearity of detection.

**CaMKII Western blot.** CAD-hNET and CAD-hNET $\Delta_{28-47}$  cells, plated at a density of  $1 \times 10^6$  cells per well, were treated in KRH/glucose buffer in the absence or presence of 10  $\mu\text{M}$  AMPH for



MOL #26690

the different time periods. The incubation was terminated on ice and the cells were washed twice with PBS/ $\text{Ca}^{2+}$ / $\text{Mg}^{2+}$  and then incubated in lysis buffer containing 20 mM Tris-HCl, pH 7.5, 1 mM EDTA, 0.5 mM PMSF, 1% SDS, 1 mM sodium orthovanadate, and 1 mM sodium pyrophosphate, 1  $\mu\text{M}$  mycrocystin-LR, and 1  $\mu\text{M}$  aproportin and leupeptin for 1 hr at 4 °C. Cell lysates were recovered by centrifugation at  $20,000 \times g$  for 30 min at 4°C. Samples were then analyzed by SDS-PAGE (10% gel) followed by immunoblotting for total and activated (phospho) CaMKII.

**Single cell calcium determinations.** For imaging intracellular  $\text{Ca}^{2+}$  changes, hNET and hNET $\Delta_{28-47}$  cells were grown for 2 days on glass cover slips (1.5 mm diameter, MatTek Corporation, Ashland MA). After washing the cells with an extracellular physiological solution (pH 7.34 and 300 mOsm, 130 mM NaCl, 1.3 mM  $\text{KH}_2\text{PO}_4$ , 0.5 mM  $\text{MgSO}_4$ , 1.5 mM  $\text{CaCl}_2$ , 10 mM HEPES, 34 mM dextrose), cells were incubated with 5  $\mu\text{M}$  Oregon Green BAPTA-AM for 20 min at room temperature in darkness and then washed 3 times. AMPH was added after the first 3-4 scanings. Images were acquired using a 488 nm excitation wavelength with a 500 long pass filter every 10 sec. To calculate  $\Delta F/F$ , for each time point, the background was subtracted (fluorescence measured from a confocal plane in the control condition (basal)) from the fluorescence recorded in the same z section upon addition of AMPH. Image analysis was performed using the public domain Image J. imaging program (<http://rsb.info.nih.gov/ij/>).

MOL #26690

## RESULTS

### **AMPH promotes a reduction in hNET surface expression, an effect enhanced in the mutant hNET $\Delta_{28-47}$ .**

To investigate the acute impact of AMPH on hNET trafficking, we studied stably transfected CAD-hNET cells exposed to 10  $\mu$ M AMPH. Figure 1A shows immunoblots obtained from biotinylated extracts from CAD-hNET cells (top blot) and from CAD-hNET $\Delta_{28-47}$  cells (bottom blot) treated either with vehicle (CTR) or with 10  $\mu$ M AMPH for the indicated time periods, with normalized quantitation of multiple biotinylation experiments shown in Fig. 1B. The inset shows immunoblots for hNET proteins obtained from total extract of CAD-hNET and CAD-hNET $\Delta_{28-47}$  cells indicating that total amount of hNET proteins is similar in these two cell lines. In CAD-hNET cells, AMPH treatment triggers a gradual, time-dependent reduction in hNET cell surface expression, achieving a nearly 50% reduction after an hour of AMPH stimulation. In contrast, in CAD-hNET $\Delta_{28-47}$  cells, AMPH rapidly triggers hNET $\Delta_{28-47}$  plasma membrane reductions, achieving a level  $50 \pm 2.7\%$  of control after only 1 min of AMPH treatment (Fig. 1B) followed by relatively little change in transporter surface expression with further AMPH exposure. One concern was that this AMPH effect on hNET $\Delta_{28-47}$  may arise from non-transporter mediated changes induced by AMPH uniquely in hNET $\Delta_{28-47}$  cells. However, pretreatment of cells with the NET antagonist desipramine (DMI) for 10 min completely blocked this AMPH effect (data not shown). To evaluate the AMPH action on hNET trafficking, NET plasma membrane proteins were assessed in preference to uptake activity due to the complex activity of AMPH pretreatment on uptake. However, to compare hNET and hNET $\Delta_{28-47}$  function, kinetic studies on [ $^3$ H]NE uptake were performed. The  $V_{\max}$  was  $12.2 \pm 0.67 \times 10^{-17}$  mol/cell/min and  $9.7 \pm 1.39 \times 10^{-17}$  mol/cell/min with a  $K_m$  of  $0.52 \pm 0.11$  and  $0.6 \pm 0.24$   $\mu$ M for CAD-hNET and CAD-hNET $\Delta_{28-47}$ , respectively. Neither the  $V_{\max}$  nor the  $K_m$  obtained from CAD-hNET cells were significantly different from those obtained from CAD-hNET $\Delta_{28-47}$  (Student *t*-test;  $p > 0.05$ ).

MOL #26690

### **AMPH increases levels of intracellular calcium.**

Since  $\text{Ca}^{2+}$  has been linked to support NET surface expression (Apparsundaram et al., 2001) and has been implicated in AMPH modulation of NET activity in PC-12 cells (Kantor et al., 2004), we investigated whether AMPH alters intracellular  $\text{Ca}^{2+}$  concentration in hNET-stably transfected CAD cells.  $\text{Ca}^{2+}$  levels were monitored using ratiometric analysis of the cell-permeant  $\text{Ca}^{2+}$  indicator, Oregon Green BAPTA-AM. Confocal microscopy images were collected at different time points and for each time point, the background (fluorescence measured from a confocal plane in control conditions (basal)) was subtracted from the fluorescence recorded in the same  $z$  section upon addition of AMPH. An increase in intracellular fluorescence was detected within 10 sec of AMPH application (Fig. 2, panel A) in both CAD-hNET and CAD-hNET $\Delta_{28-47}$  cells. However, the time course and magnitude of effects was quite distinct. The relative changes ( $\Delta F/F$ ) in  $\text{Ca}^{2+}$  sensitive fluorescence was significantly more rapid and achieved higher levels in CAD-hNET $\Delta_{28-47}$  cells as compared to CAD-hNET cells (Fig. 2, panel B). No significant changes in intracellular fluorescence were detected either in CAD cells treated with AMPH or in vehicle treated hNET and hNET $\Delta_{28-47}$  cells (data not shown). Importantly, these increases in intracellular  $\text{Ca}^{2+}$  were blocked by pretreatment with either 50  $\mu\text{M}$   $\text{Cd}^{2+}$  or 10  $\mu\text{M}$  DMI (data not show) indicating, therefore, that this AMPH effect requires both  $\text{Ca}^{2+}$  channel activation and possibly NET activity. Also, these data suggest that the differences noticed in the AMPH-induced cell surface redistribution of hNET vs hNET $\Delta_{28-47}$  may be supported by  $\text{Ca}^{2+}$  sensitive mechanisms.

### **AMPH-induced changes in hNET cell surface redistribution are $\text{Ca}^{2+}$ dependent.**

The ability of AMPH to promote a greater increase in intracellular  $\text{Ca}^{2+}$  in CAD-hNET $\Delta_{28-47}$  cells with respect to CAD-hNET cells that is temporally correlated with accelerated changes in transporter cell surface redistribution raises the possibility that these two phenomena are related. We therefore asked whether rapid AMPH-induced hNET $\Delta_{28-47}$  trafficking is impaired by either blocking plasma membrane  $\text{Ca}^{2+}$  channel activity with  $\text{Cd}^{2+}$  or by buffering the increase in

MOL #26690

intracellular  $\text{Ca}^{2+}$  with BAPTA-AM. Figure 3A, top blot, shows a representative immunoblot for hNET proteins recovered from the biotinylated fraction obtained from hNET $\Delta_{28-47}$  cells treated either with vehicle (CTR), with 10  $\mu\text{M}$  AMPH for 1 min (AMPH), with 50  $\mu\text{M}$   $\text{Cd}^{2+}$  for 30 sec ( $\text{Cd}^{2+}$ ), or with 50  $\mu\text{M}$   $\text{Cd}^{2+}$  for 30 sec followed by 10  $\mu\text{M}$  AMPH for 1 min in the continuous presence of  $\text{Cd}^{2+}$  ( $\text{Cd}^{2+}$  + AMPH). An immunoblot for hNET proteins recovered from total extracts is represented in Fig. 3A, bottom blot. Figure 3B, top blot, shows a representative immunoblot for hNET proteins recovered from the biotinylated fraction obtained from hNET $\Delta_{28-47}$  cells incubated in a  $\text{Ca}^{2+}$  free buffer and treated with vehicle (CTR), with 50  $\mu\text{M}$  BAPTA-AM (BAPTA) for 40 min, or with 50  $\mu\text{M}$  BAPTA-AM for 40 min followed by 10  $\mu\text{M}$  AMPH for 1 min in the continuous presence of BAPTA-AM (BAPTA+ AMPH). An immunoblot for hNET proteins recovered from total extracts is represented in Fig. 3B, bottom blot. As shown in the bar graphs in Figures 3C-D, both treatments completely blocked the ability of AMPH to trigger loss of transporters from the cell surface.

### **AMPH induces rapid CaMKII activation and, as a consequence, causes hNET $\Delta_{28-47}$ cell surface redistribution.**

Next we considered whether AMPH-induced changes in intracellular  $\text{Ca}^{2+}$  are significant enough to modify activity of  $\text{Ca}^{2+}$ -dependent kinases. We focused on CaMKII due to studies indicating an inhibitory action of calmodulin antagonists on NET activity as well as suggestions that CaMKII may phosphorylate NET (Uchida et al., 1998). Using a phosphospecific antibody produced against a synthetic phosphopeptide corresponding to amino acid residues surrounding the phosphorylated Thr286 (the autophosphorylation site associated with CaMKII activation), we examined the AMPH effects on CaMKII activation. Figure 4A shows an immunoblot of Thr286 phospho-CaMKII (CaMKII-P) after treatment of CAD-hNET $\Delta_{28-47}$  cells with vehicle (CTR) or with 10  $\mu\text{M}$  AMPH (AMPH) for 1 or 10 min. Figure 4B shows quantification of the band density of three different experiments as in panel A, normalized to control conditions. AMPH rapidly increases the level of CaMKII phosphorylation, with

MOL #26690

significant effects observed after as little as 1 min of AMPH addition. No changes were observed in total levels of CaMKII as assessed with a non-phosphospecific CaMKII antibody (data not shown).

It is possible that the ability of AMPH to increase levels of CaMKII phosphorylation arises from non-transporter-mediated changes induced by AMPH in hNET $\Delta_{28-47}$  cells. However, pretreatment of CAD-hNET $\Delta_{28-47}$  cells with 10  $\mu$ M DMI for 10 min completely blocked this AMPH effect. In the presence of DMI, AMPH increased the level of CaMKII phosphorylation to  $105 \pm 3$  % of control conditions (n=3).

To assess a requirement for CaMKII stimulation in AMPH trigger changes in hNET $\Delta_{28-47}$  cell surface redistribution, we performed biotinylation experiments in the presence or absence of the CaMKII inhibitor KN93, preapplied in the bath solution prior to AMPH application. Figure 4C shows representative immunoblots for hNET $\Delta_{28-47}$  proteins recovered from the biotinylated fraction (top blot) and total extract (bottom blot) of CAD-hNET $\Delta_{28-47}$  cells treated either with vehicle (CTR), with 10  $\mu$ M AMPH for 1 min (AMPH), with 10  $\mu$ M KN93 for 30 min (KN93), or with 10  $\mu$ M KN93 for 30 min followed by 10  $\mu$ M AMPH for 1 min in the continuous presence of KN93 (KN93 + AMPH). As quantitated in Figure 4D, preincubation of hNET $\Delta_{28-47}$  cell with KN93 blocked the ability of AMPH to cause hNET $\Delta_{28-47}$  cell surface redistribution, supporting a role of CaMKII in this AMPH action. In contrast to KN93, the inactive analog KN92 had no significant effect (data not shown).

### **Acute AMPH regulates NET/SYN1A interaction**

SYN1A colocalizes with NET at noradrenergic varicosities (Sung et al., 2003) and associates with NET in heterologous expression systems and native tissues (Sung et al., 2003). Since SYN1A supports the surface trafficking of NET proteins (Sung et al., 2003), we considered whether AMPH is able to alter NET/SYN1A associations and whether differences exist between hNET and hNET $\Delta_{28-47}$ . For these studies, we transiently transfected CAD cells either with SYN1A cDNAs, with tagged hNET cDNAs, or with both, and then treated these cells either with vehicle or

MOL #26690

AMPH followed by biotinylation and NET/SYN1A co-immunoprecipitation. His and HA antibodies failed to immunoprecipitate SYN1A from untransfected cells. In contrast, SYN1A was detected in immunoprecipitates from total extracts of CAD cells cotransfected with SYN1A and with His-hNET cDNA (Fig 5A). After 1 min treatment, AMPH (10  $\mu$ M) increased hNET/SYN1A interactions at the plasma membrane (Fig. 5A-B) with respect to control conditions. In contrast, the hNET/SYN1A interactions recovered from the nonbiotinylated fractions were unaffected by AMPH treatment. AMPH increased hNET/SYN1A complexes at the plasma membrane to  $130 \pm 11$  % of vehicle treated control. Similarly, SYN1A was detected in immunoprecipitates from total extracts of CAD cells cotransfected with SYN1A and with HA-hNET $\Delta_{28-47}$  cDNA (Fig 5C). Consistent with studies with hNET, AMPH (10  $\mu$ M) treatment (1 min) increased hNET $\Delta_{28-47}$ /SYN1A interactions at the plasma membrane (Fig. 5C) with respect to vehicle treated control. Similarly, the intracellular hNET $\Delta_{28-47}$ /SYN1A interactions were slightly but not significantly affected by AMPH treatment (Fig. 5C-D). Compared to hNET experiments, AMPH increased hNET $\Delta_{28-47}$ /SYN1A complexes at the plasma membrane to a greater extent, with an increase of  $191 \pm 26$  % of vehicle treated control. These findings indicate that the AMPH-induced rapid hNET $\Delta_{28-47}$  trafficking correlates with more extensive NET/SYN1A interactions.

### **CaMKII inhibition attenuates recovery of increased plasma membrane SYN1A/hNET $\Delta_{28-47}$ complexes**

Although Figure 5 demonstrates that AMPH robustly increases hNET $\Delta_{28-47}$ /SYN1A associations at the plasma membrane to a greater extent than hNET/SYN1A complexes and this phenomenon appears to correlate with increases of intracellular Ca<sup>2+</sup>, these effects could represent parallel and possibly unrelated actions of AMPH. Interestingly, the time required to demonstrate an increase in hNET $\Delta_{28-47}$ /SYN1A association is similar to the time required by AMPH to cause hNET $\Delta_{28-47}$  cell surface redistribution. Consequently, we considered that stabilization of hNET $\Delta_{28-47}$ /SYN1A complexes may be a step of the AMPH-induced NET cell surface redistribution pathway.

MOL #26690

Because the ability of AMPH to promote a decreased hNET $\Delta_{28-47}$  plasma membrane expression is impaired by CaMKII inhibition with KN93 (Fig. 4), we asked whether KN93 treatment could block the AMPH-induced increase in hNET $\Delta_{28-47}$ /SYN1A associations. CAD cells cotransfected with SYN1A and with HA-hNET $\Delta_{28-47}$  cDNA were treated either with vehicle (CTR) or with 10  $\mu$ M KN93 for 30 min followed by 10  $\mu$ M AMPH for 1 min in the continued presence of KN93 (KN93 + AMPH) (Fig. 6). As before, blots of total extracts also show no impact of AMPH on SYN1A content. However, we found that KN93 treatment blocked the ability of AMPH to increase plasma hNET $\Delta_{28-47}$ /SYN1A complexes (HA IP-surf/AMPH+KN93) with respect to control conditions (Fig. 6A). Interestingly, because the intracellular hNET $\Delta_{28-47}$ /SYN1A interactions were unaffected by AMPH treatment (Fig. 5 C-D), these data suggest that CaMKII mechanisms target NET/SYN1A complexes in a compartmentally specific-fashion.

MOL #26690

## DISCUSSION

Neurotransmitter transporters are increasingly recognized as highly regulated components of synaptic signaling, responding to coincident neuronal activation and/or receptor activation to modulate both of the number of active carriers at the plasma membrane and the rates of transport through individual transporters (Gonzalez and Robinson, 2004; Blakely, 2005; Kahlig and Galli, 2003; Robinson, 2001; Torres, 2006). Multiple signaling pathways have been implicated in the regulation of catecholamine transporter trafficking and catalytic function including pathways linked to PKC, PI3K, CaMKII, p38 MAPK and PP2A (Bauman et al., 2000; Blakely et al., 2005; Blakely and Sung, 2000; Gonzalez and Robinson, 2004; Kahlig and Galli, 2003; Robinson, 2001; Torres, 2006). Transporter-associated proteins are thought to play an important role in the transduction of activated signaling pathways to alter transporter localization and function. The NET interacts, among others, with cytosolic scaffolding proteins such as the PDZ domain protein PICK1 (Torres et al., 2001) as well as with other intrinsic membrane proteins, most prominent of which is the t-SNARE protein SYN1A (Sung et al., 2003). In prior studies, we demonstrated that SYN1A supports cell-surface trafficking of hNET as well as that direct associations between NET and SYN1A influence hNET electrical activity (Sung et al., 2003). The degree to which NET substrates and antagonists influence these associations is unknown, although a precedent exists for both substrate and antagonist influences on localization and regulation of homologous DAT (Daws et al., 2002; Kahlig et al., 2004; Saunders et al., 2000) and SERT proteins (Ramamoorthy and Blakely, 1999).

In heterologous expression systems as well as in *ex vivo* preparations, AMPH exposure diminishes plasma membrane expression of DAT proteins (Chi and Reith, 2003; Gulley et al., 2002; Saunders et al., 2000). Moreover, AMPH acting through either DAT or NET proteins has been reported to promote an increase in intracellular  $\text{Ca}^{2+}$  mediated by activation of voltage-sensitive



MOL #26690

Ca<sup>2+</sup> channels (Gnegy et al., 2004; Kantor et al., 2004). In the current study, we demonstrate that AMPH triggers a redistribution of hNET cell surface proteins in concert with an accumulation of plasma membrane hNET/SYN1A complexes, actions supported by an elevation of intracellular Ca<sup>2+</sup> and CaMKII activation. This phenomenon appears distinct from phorbol ester or muscarinic receptor-triggered hNET internalization, where the NET internalization is accompanied by a reduction in hNET/SYN1A associations and it is sensitive to PKC antagonists (Apparsundaram et al., 1998; Sung et al., 2003).

In order to study the molecular mechanism supporting AMPH-induced hNET trafficking, we took advantage of the comparatively more rapid AMPH-induced trafficking induced in hNET $\Delta_{28-47}$  as compared to hNET transfected cells. Here, we show that a deletion of a region of 20 amino acids ( $\Delta_{28-47}$ ) from the hNET N-terminus increases the rate at which AMPH causes significant cell surface redistribution of hNET $\Delta_{28-47}$  (Fig. 1). Importantly, the hNET  $\Delta_{28-47}$  deletion does not disrupt hNET/SYN1A associations, but may actually enhance them as we captured larger AMPH-induced changes in hNET/SYN1A complexes than could be observed with hNET. Alternatively, the initiating events leading to SYN1A/hNET associations may be enhanced in hNET $\Delta_{28-47}$ . In support of this idea, AMPH caused a significantly larger increase in intracellular Ca<sup>2+</sup> in CAD-hNET $\Delta_{28-47}$  cells as compared to CAD-hNET cells (Fig. 2). This was not due to higher levels of transporter expression since our stable CAD-hNET $\Delta_{28-47}$  cells express transporter proteins at the same level than our CAD-hNET cells. Possibly, hNET $\Delta_{28-47}$  is permissive for a greater degree of AMPH-induced membrane depolarization, triggering a more robust opening of Ca<sup>2+</sup> channels. Substrate-induced currents through neurotransmitter transporters are known to be sufficient to depolarize cell membranes (Carvelli et al., 2004; Ingram et al., 2002; Kahlig et al., 2004). Elimination of SYN1A interactions through mutation of a distinct area of the hNET NH2 terminus (Binda et al., 2005) generates a greatly enhanced hNET leak current, supporting contributions of this domain to transporter conductance states that may also come into play with respect to the more robust

MOL #26690

response to AMPH seen with hNET $\Delta_{28-47}$ . Importantly, we found that Cd<sup>2+</sup>, a non specific Ca<sup>2+</sup> channel blocker (Kim et al., 1998; Mesquita et al., 1998), significantly reduced the ability of AMPH to increase intracellular Ca<sup>2+</sup> (data not shown) and to cause hNET $\Delta_{28-47}$  cell surface redistribution (Fig. 3A). Moreover, chelation of intracellular Ca<sup>2+</sup> with BAPTA-AM blocked AMPH-induced reduction in hNET $\Delta_{28-47}$  cell surface expression (Fig. 3), suggesting both that AMPH-induced NET ion flux triggers activation of voltage-sensitive Ca<sup>2+</sup> channels that in turn support changes in hNET $\Delta_{28-47}$  cell surface redistribution and SYN1A associations. A similar sequence of events is evident with hNET, though at a reduced rate and extent. Therefore, it seems likely that other cellular events could act in concert with AMPH to determine the more rapid modulation exhibited constitutively by hNET $\Delta_{28-47}$ .

Using the more robustly regulated CAD-hNET $\Delta_{28-47}$  cells, we found that AMPH increases CaMKII phosphorylation within 1 min of AMPH application. Like hNET trafficking changes, CaMKII activation was blocked by preincubation with Cd<sup>2+</sup> prior to AMPH stimulation (data not shown), suggesting that activation of CaMKII activity is essential to the modulation of hNET by the psychostimulant. This is supported by the ability of KN93 to block AMPH-induced hNET trafficking. That AMPH triggered SYN1A associations are also blocked by KN93 suggests that these associations either support internalization or represent a parallel action. For example, it is possible that CaMKII activity enhances hNET/SYN1A associations independently of its ability to cause hNET cell surface redistribution. Further studies are needed to distinguish between these possibilities.

Our findings of a role for CaMKII in AMPH-induced NET internalization are at apparent odds with studies of Uchida and coworkers (Uchida et al., 1998) who reported that elevated external Ca<sup>2+</sup> elevated NET function in a KN93 sensitive manner. Important distinctions between our studies and those of Uchida and coworkers are worth noting. For example, Uchida and coworkers used PC12 cells for their studies that are derived from rat pheochromocytoma and, as such, are of

MOL #26690

adrenal medullary origin. Instead, CAD cells are of CNS origin. Also, we used AMPH as the stimulus for NET regulation as opposed to  $\text{Ca}^{2+}$  manipulations in the medium, and, as such, binding and/or translocation of AMPH itself may place the transporter in a distinct conformation favoring internalization. Alternatively, the magnitude and timing of  $\text{Ca}^{2+}$  changes induced by these two experimental paradigms may be distinct. In neurons, for example, it is known that both exocytosis and endocytosis exhibit  $\text{Ca}^{2+}$  dependence (Kuromi et al., 2004). In parallel, NET inward and outward trafficking can both be influenced by  $\text{Ca}^{2+}$ /CaMKII dependent mechanisms, with the final outcome determined by more subtle changes in transporter-ligand interactions, rates of rise of  $\text{Ca}^{2+}$  and/or compartmentalization of  $\text{Ca}^{2+}$ /CaMKII. In support of multiple  $\text{Ca}^{2+}$ -mediated mechanisms regulating NET trafficking, we found that manipulations that engender elevations in internal  $\text{Ca}^{2+}$  in the absence of AMPH diminish hNET/SYN1A associations (Sung *et al.*, manuscript in preparation). Our findings with hNET $\Delta_{28-47}$  suggest that sequences in the hNET NH2 terminus may be responsible for a bidirectional response to changes in intracellular  $\text{Ca}^{2+}$  such that with their removal, a more profound bias toward internalization emerges. For example, it is possible that in hNET $\Delta_{28-47}$ , we deleted CaMKII phosphorylation sites regulating hNET/SYN1A associations. Indeed, it has been shown for the homologous DAT that the NH2 terminus is a target of phosphorylation of CaMKII (Fog et al., 2006). Future studies can target specific sequences within this domain to probe the intersecting pathways that ultimately set levels of cell surface transporter protein and NE clearance capacity.

In summary, we document that the ability of AMPH to trigger the internalization of hNET is dependent on AMPH-induced changes in intracellular  $\text{Ca}^{2+}$  and CaMKII activation. The differences that we observe in rate and magnitude of responses between hNET and hNET $\Delta_{28-47}$  reveal how changes in transporter sequence, as might arise through naturally occurring transporter gene variants, can influence transporter regulation in response to identical regulatory contexts (Hahn et al., 2005; Mazei-Robison and Blakely, 2005; Mazei-Robison et al., 2005; Prasad et al., 2005). It also seems reasonable to speculate that alterations in levels or activity of transporter regulatory

MOL #26690

proteins or their upstream modulators that ultimately impact the hNET NH<sub>2</sub> terminus could mimic these differences. Thus, knowledge of these regulatory mechanisms could provide new insights for understanding altered responsiveness of catecholamine transporters following repeated AMPH administration (Iwata et al., 1997; Kantor et al., 2004).

## References

- Apparsundaram S, Galli A, DeFelice LJ, Hartzell HC and Blakely RD (1998) Acute regulation of norepinephrine transport: I. protein kinase C-linked muscarinic receptors influence transport capacity and transporter density in SK-N-SH cells. *Journal of Pharmacology & Experimental Therapeutics* **287**:733-743.
- Apparsundaram S, Sung UH, Price RD and Blakely RD (2001) Trafficking-dependent and -independent pathways of neurotransmitter transporter regulation differentially involving p38 mitogen-activated protein kinase revealed in studies of insulin modulation of norepinephrine transport in SK-N-SH cells. *Journal of Pharmacology & Experimental Therapeutics* **299**:666-677.
- Bauman AL, Apparsundaram S, Ramamoorthy S, Wadzinski BE, Vaughan RA and Blakely RD (2000) Cocaine and antidepressant-sensitive biogenic amine transporters exist in regulated complexes with protein phosphatase 2A. *J Neurosci* **20**:7571-7578.
- Beckman ML and Quick MW (1998) Neurotransmitter transporters: regulators of function and functional regulation. *Journal of Membrane Biology* **164**:1-10.
- Binda F, Lute BJ, Dipace C, Blakely RD and Galli A (2005) The N-terminus of the norepinephrine transporter regulates the magnitude and selectivity of the transporter-associated leak current. *Neuropharmacology*.
- Blakely RD, Defelice LJ and Galli A (2005) Biogenic amine neurotransmitter transporters: just when you thought you knew them. *Physiology (Bethesda)* **20**:225-231.
- Blakely RD and Sung U (2000) SNARE-ing neurotransmitter transporters. *Nat Neurosci* **3**:969-971.
- Burnette WB, Bailey MD, Kukoyi S, Blakely RD, Trowbridge CG and Justice JB, Jr. (1996) Human norepinephrine transporter kinetics using rotating disk electrode voltammetry. *Analytical Chemistry* **68**:2932-2938.
- Carvelli L, McDonald PW, Blakely RD and Defelice LJ (2004) Dopamine transporters depolarize neurons by a channel mechanism. *Proc Natl Acad Sci U S A* **101**:16046-16051.
- Cervinski MA, Foster JD and Vaughan RA (2005) Psychoactive substrates stimulate dopamine transporter phosphorylation and down regulation by cocaine sensitive and protein kinase C dependent mechanisms. *J Biol Chem*.
- Chi L and Reith ME (2003) Substrate-induced trafficking of the dopamine transporter in heterologously expressing cells and in rat striatal synaptosomal preparations. *J Pharmacol Exp Ther* **307**:729-736.
- Daws LC, Callaghan PD, Moron JA, Kahlig KM, Shippenberg TS, Javitch JA and Galli A (2002) Cocaine increases dopamine uptake and cell surface expression of dopamine transporters. *Biochem Biophys Res Commun* **290**:1545-1550.
- Deken SL, Beckman ML, Boos L and Quick MW (2000) Transport rates of GABA transporters: regulation by the N-terminal domain and syntaxin 1A. *Nat Neurosci* **3**:998-1003.
- Fleckenstein AE, Haughey HM, Metzger RR, Kokoshka JM, Riddle EL, Hanson JE, Gibb JW and Hanson GR (1999) Differential effects of psychostimulants and related agents on dopaminergic and serotonergic transporter function. *European Journal of Pharmacology* **382**:45-49.
- Fog JU, Khoshbouei H, Holy M, Owens WA, Vaegter CB, Sen N, Nikandrova Y, Bowton E, McMahon DG, Colbran RJ, Daws LC, Sitte HH, Javitch JA, Galli A and Gether U (2006) Calmodulin Kinase II Interacts with the Dopamine Transporter C Terminus to Regulate Amphetamine-Induced Reverse Transport. *Neuron* **51**:417-429.
- Garcia BG, Wei Y, Moron JA, Lin RZ, Javitch JA and Galli A (2005) Akt is essential for insulin modulation of amphetamine-induced human dopamine transporter cell-surface redistribution. *Mol Pharmacol* **68**:102-109.

MOL #26690

- Gnegy ME, Khoshbouei H, Berg KA, Javitch JA, Clarke WP, Zhang M and Galli A (2004) Intracellular Ca<sup>2+</sup> regulates amphetamine-induced dopamine efflux and currents mediated by the human dopamine transporter. *Mol Pharmacol* **66**:137-143.
- Gonzalez MI and Robinson MB (2004) Neurotransmitter transporters: why dance with so many partners? *Curr Opin Pharmacol* **4**:30-35.
- Gulley JM, Doolen S and Zahniser NR (2002) Brief, repeated exposure to substrates down-regulates dopamine transporter function in *Xenopus* oocytes in vitro and rat dorsal striatum in vivo. *J Neurochem* **83**:400-411.
- Hahn MK, Mazei-Robison MS and Blakely RD (2005) Single nucleotide polymorphisms in the human norepinephrine transporter gene affect expression, trafficking, antidepressant interaction, and protein kinase C regulation. *Mol Pharmacol* **68**:457-466.
- Ingram SL, Prasad BM and Amara SG (2002) Dopamine transporter-mediated conductances increase excitability of midbrain dopamine neurons. *Nat Neurosci* **5**:971-978.
- Iversen LL (1971) Role of transmitter uptake mechanisms in synaptic neurotransmission. *British Journal of Pharmacology* **41**:571-591.
- Iwata SI, Hewlett GH, Ferrell ST, Kantor L and Gnegy ME (1997) Enhanced dopamine release and phosphorylation of synapsin I and neuromodulin in striatal synaptosomes after repeated amphetamine. *Journal of Pharmacology & Experimental Therapeutics* **283**:1445-1452.
- Jayanthi LD, Samuvel DJ and Ramamoorthy S (2004) Regulated internalization and phosphorylation of the native norepinephrine transporter in response to phorbol esters: Evidence for localization in lipid rafts and lipid raft mediated internalization. *J Biol Chem*.
- Johnson LA, Furman CA, Zhang M, Guptaroy B and Gnegy ME (2005) Rapid delivery of the dopamine transporter to the plasmalemmal membrane upon amphetamine stimulation. *Neuropharmacology* **49**:750-758.
- Kahlig KM and Galli A (2003) Regulation of dopamine transporter function and plasma membrane expression by dopamine, amphetamine, and cocaine. *Eur J Pharmacol* **479**:153-158.
- Kahlig KM, Javitch JA and Galli A (2004) Amphetamine regulation of dopamine transport. Combined measurements of transporter currents and transporter imaging support the endocytosis of an active carrier. *J Biol Chem* **279**:8966-8975.
- Kantor L, Zhang M, Guptaroy B, Park YH and Gnegy ME (2004) Repeated amphetamine couples norepinephrine transporter and calcium channel activities in PC12 cells. *J Pharmacol Exp Ther* **311**:1044-1051.
- Kim SJ, Sung JJ and Park YS (1998) L-type and dihydropyridine-resistant calcium channel trigger exocytosis with similar efficacy in single rat pancreatic beta cells. *Biochem Biophys Res Commun* **243**:878-884.
- Kuromi H, Honda A and Kidokoro Y (2004) Ca(2+) Influx through Distinct Routes Controls Exocytosis and Endocytosis at *Drosophila* Presynaptic Terminals. *Neuron* **41**:101-11.
- Lu D, Yang H, Lenox RH and Raizada MK (1998) Regulation of angiotensin II-induced neuromodulation by MARCKS in brain neurons. *J Cell Biol* **142**:217-227.
- Lu D, Yu K, Paddy MR, Rowland NE and Raizada MK (1996) Regulation of norepinephrine transport system by angiotensin II in neuronal cultures of normotensive and spontaneously hypertensive rat brains. *Endocrinology* **137**:763-772.
- Mazei-Robison MS and Blakely RD (2005) Expression studies of naturally occurring human dopamine transporter variants identifies a novel state of transporter inactivation associated with Val382Ala. *Neuropharmacology* **49**:737-749.
- Mazei-Robison MS, Couch RS, Shelton RC, Stein MA and Blakely RD (2005) Sequence variation in the human dopamine transporter gene in children with attention deficit hyperactivity disorder. *Neuropharmacology* **49**:724-736.
- Mesquita F, Jr., Prado MA, Gomez RS, Romano-Silva MA and Gomez MV (1998) The effect of calcium channels blockers in the K<sup>+</sup>-evoked release of [3H]adenine nucleotides from rat brain cortical synaptosomes. *Neurosci Lett* **258**:57-59.

MOL #26690

- Pacholczyk T, Blakely RD and Amara SG (1991) Expression cloning of a cocaine- and antidepressant-sensitive human noradrenaline transporter. *Nature* **350**:350-354.
- Pifl C and Singer EA (1999) Ion dependence of carrier-mediated release in dopamine or norepinephrine transporter-transfected cells questions the hypothesis of facilitated exchange diffusion. *Molecular Pharmacology* **56**:1047-1054.
- Prasad HC, Zhu CB, McCauley JL, Samuvel DJ, Ramamoorthy S, Shelton RC, Hewlett WA, Sutcliffe JS and Blakely RD (2005) Human serotonin transporter variants display altered sensitivity to protein kinase G and p38 mitogen-activated protein kinase. *Proc Natl Acad Sci U S A* **102**:11545-11550.
- Qi Y, Wang JK, McMillian M and Chikaraishi DM (1997) Characterization of a CNS cell line, CAD, in which morphological differentiation is initiated by serum deprivation. *J Neurosci* **17**:1217-1225.
- Quick MW (2003) Regulating the conducting states of a mammalian serotonin transporter. *Neuron* **40**:537-549.
- Ramamoorthy S and Blakely RD (1999) Phosphorylation and sequestration of serotonin transporters differentially modulated by psychostimulants. *Science* **285**:763-766.
- Robinson MB (2001) Regulated trafficking of neurotransmitter transporters: common notes but different melodies. *Journal of Neurochemistry* **78**:276-286.
- Saunders C, Ferrer JV, Shi L, Chen J, Merrill G, Lamb ME, Leeb-Lundberg LM, Carvelli L, Javitch JA and Galli A (2000) Amphetamine-induced loss of human dopamine transporter activity: an internalization-dependent and cocaine-sensitive mechanism. *Proc Natl Acad Sci U S A* **97**:6850-6855.
- Sung U, Apparsundaram S, Galli A, Kahlig KM, Savchenko V, Schroeter S, Quick MW and Blakely RD (2003) A regulated interaction of syntaxin 1A with the antidepressant-sensitive norepinephrine transporter establishes catecholamine clearance capacity. *J Neurosci* **23**:1697-1709.
- Tatsumi M, Groshan K, Blakely RD and Richelson E (1997) Pharmacological profile of antidepressants and related compounds at human monoamine transporters. *Eur J Pharmacol* **340**:249-258.
- Torres GE (2006) The dopamine transporter proteome. *J Neurochem*.
- Torres GE, Yao WD, Mohn AR, Quan H, Kim KM, Levey AI, Staudinger J and Caron MG (2001) Functional interaction between monoamine plasma membrane transporters and the synaptic PDZ domain-containing protein PICK1. *Neuron* **30**:121-134.
- Trendelenburg U (1991) The TiPS lecture: functional aspects of the neuronal uptake of noradrenaline. *Trends in Pharmacological Sciences* **12**:334-337.
- Uchida J, Kiuchi Y, Ohno M, Yura A and Oguchi K (1998) Ca(2+)-dependent enhancement of [3H]noradrenaline uptake in PC12 cells through calmodulin-dependent kinases. *Brain Res* **809**:155-164.
- Wall SC, Gu H and Rudnick G (1995) Biogenic amine flux mediated by cloned transporters stably expressed in cultured cell lines: amphetamine specificity for inhibition and efflux. *Molecular Pharmacology* **47**:544-550.
- Wang D, Deken SL, Whitworth TL and Quick MW (2003) Syntaxin 1A inhibits GABA flux, efflux, and exchange mediated by the rat brain GABA transporter GAT1. *Mol Pharmacol* **64**:905-913.
- Yamashita A, Singh SK, Kawate T, Jin Y and Gouaux E (2005) Crystal structure of a bacterial homologue of Na<sup>+</sup>/Cl<sup>-</sup>-dependent neurotransmitter transporters. *Nature* **437**:215-223.
- Yang H and Raizada MK (1998) MAP kinase-independent signaling in angiotensin II regulation of neuromodulation in SHR neurons. *Hypertension* **32**:473-481.

MOL #26690

## FOOTNOTES

This work was supported by NIH grants MH058921 and DA 14684 (A.G).

RDB and AG contributed equally to this work



MOL #26690

## FIGURE LEGENDS

**Figure 1. A region of 20 amino acids ( $\Delta_{28-47}$ ) of the hNET N-terminus regulates AMPH-induced hNET cell surface redistribution.** (A) Representative immunoblots for hNET proteins recovered from biotinylated extracts obtained from hNET (top blot) and hNET $\Delta_{28-47}$  (bottom blot) cells treated with 10  $\mu$ M AMPH for the indicated periods of time. (B) Quantification of the immunoblots using the Scion Image System. The density of the biotinylated samples was normalized to the density of the parallel total extract in order to correct for difference in cell seeding and hNET expression in different wells and expressed as percentage of control. The normalized data (closed squares for hNET, open circles for hNET $\Delta_{28-47}$ ) are expressed as mean  $\pm$  SEM and compared to respective controls by one way ANOVA followed by the Dunett's test; \* ; # = level of significance  $p < 0.001$ ;  $n=4$ . Inset: Representative immunoblot for hNET and hNET $\Delta_{28-47}$  proteins recovered from total extract under control conditions.

**Figure 2. AMPH induces a larger increase in intracellular  $\text{Ca}^{2+}$  in hNET $\Delta_{28-47}$  cells with respect to hNET cells.** (A) Intracellular  $\text{Ca}^{2+}$  fluorescence was acquired using confocal imaging from hNET and hNET $\Delta_{28-47}$  cells.  $\text{Ca}^{2+}$  green fluorescence was measured from a z section of the cell and used to monitor temporal changes of intracellular  $\text{Ca}^{2+}$  levels upon AMPH application. To determine AMPH-induced changes in fluorescence, the background fluorescence (BASAL) was subtracted from each single time point including control conditions (REST). Upon AMPH application (AMPH), an increase of intracellular fluorescence was detected as a function of time, as measured in seconds. (B) The relative changes ( $\Delta F/F$ ) in  $\text{Ca}^{2+}$  sensitive fluorescence induced by AMPH were evaluated by Image J. imaging analysis. The images were collected every 10 sec for the indicated period of time. The ratio  $\Delta F/F$  was measured for hNET $\Delta_{28-47}$  (open circles) and hNET cells (closed squares)( $n = 3$ ) for each time point. The normalized data are expressed as mean  $\pm$  SEM

MOL #26690

and compared to respective controls by one way ANOVA followed by Dunnett's test (\*, # = level of significance  $p < 0.001$ ).

**Figure 3.  $\text{Cd}^{2+}$  and BAPTA-AM block the AMPH-induced hNET $\Delta_{28-47}$  trafficking.**

(A) Representative immunoblot for hNET proteins recovered from biotinylated fraction obtained from hNET $\Delta_{28-47}$  cells treated with vehicle (CTR), with 10  $\mu\text{M}$  AMPH for 1 min (AMPH), with 50  $\mu\text{M}$   $\text{Cd}^{2+}$  for 30 sec ( $\text{Cd}^{2+}$ ), or with 50  $\mu\text{M}$   $\text{Cd}^{2+}$  for 30 sec followed by 10  $\mu\text{M}$  AMPH for 1 min in the continuous presence of  $\text{Cd}^{2+}$  ( $\text{Cd}^{2+}$  + AMPH). (B) Representative immunoblot for hNET proteins recovered from the biotinylated fraction obtained from hNET $\Delta_{28-47}$  cells incubated in a  $\text{Ca}^{2+}$  free buffer and treated with vehicle (CTR), with 50  $\mu\text{M}$  BAPTA-AM (BAPTA) for 40 min, or with 50  $\mu\text{M}$  BAPTA-AM for 40 min followed by 10  $\mu\text{M}$  AMPH for 1 min in the continuous presence of BAPTA-AM (BAPTA + AMPH). (C, D) Quantification of the density of the immunoblots of panels A and B respectively, using Scion Image system. The density of the biotinylated samples was normalized to the parallel total extracts and expressed as a percentage of vehicle treated control. The normalized data are expressed as mean  $\pm$  SEM and compared against respective controls by one way ANOVA followed by Dunnett's test ( $n=4$ ; \* = level of significance  $p < 0.001$ ).

**Figure 4. AMPH and CaMKII activation induce hNET $\Delta_{28-47}$  trafficking.**

Panel A shows an immunoblot of phosphorylated CaMKII (CaMKII-p) obtained from hNET $\Delta_{28-47}$  cells treated either with vehicle (CTR) or 10  $\mu\text{M}$  AMPH for the indicated periods of time. Panel B shows quantitation of the band density of three different experiments as in panel A, normalized to control conditions. The normalized data are expressed as mean  $\pm$  SEM and compared against respective controls by one way ANOVA followed by Dunnett's test ( $n=3$ ; \* = level of significance  $p < 0.001$ ). (C) Representative immunoblot for hNET proteins recovered from biotinylated and total fraction obtained from hNET $\Delta_{28-47}$  cells treated with vehicle (CTR), with 10  $\mu\text{M}$  AMPH for 1 min (AMPH),

MOL #26690

with 10  $\mu$ M KN93 for 30 min (KN93), or with 10  $\mu$ M KN93 for 30 min followed by 10  $\mu$ M AMPH for 1 min in the continuous presence of KN93 (KN93 + AMPH). (D) Quantitation of the band density as panels A using Scion Image system. The density of the biotinylated samples was normalized to the parallel total extracts and expressed as a percentage of vehicle treated control. The normalized data are expressed as mean  $\pm$  SEM and compared against respective controls by one way ANOVA followed by Dunnett's test ( $n=3$ ; \* = level of significance  $p < 0.001$ ).

**Figure 5. AMPH-induced increase in hNET/SYN1A association occurs within plasma membrane localized complexes and it is larger in hNET $\Delta_{28-47}$  cells with respect to hNET cells.**

(A) CAD cells, cotransfected both with His-hNET and SYN1A, were treated either with vehicle (CTR) or 10  $\mu$ M AMPH for 1 min. Surface proteins were labeled with NHS-sulfo-biotin at 4  $^{\circ}$ C before cell lysis and then recovered by using avidin beads. Bound hNET proteins were immunoprecipitated with anti-His antibody and resolved on SDS-PAGE, and immunoblotted (WB:SYN1A) for SYN1A (His IP-surf). Nonbound extracts were immunoprecipitated and blotted in parallel (His IP-intra). Blots obtained from total extracts (Total) show no impact of AMPH on SYN1A content. (B) The density of the immunoprecipitates bands (His IP-surf and His IP-intra) was normalized to the density of the correspondent parallel total extract and expressed as percentage of respective control. The normalized data are expressed as mean  $\pm$  SEM and compared to respective controls by Student *t*-test; \* = level of significance  $p < 0.05$ ;  $n=3$ . (C) CAD cells, cotransfected with HA-hNET $\Delta_{28-47}$  and SYN1A, were treated either with vehicle (CTR) or 10  $\mu$ M AMPH for 1 min. Surface proteins were labeled as described in panel A. Surface complexes were recovered using avidin beads. Bound HA-hNET $\Delta_{28-47}$  proteins were immunoprecipitated with anti-HA and resolved on SDS-PAGE, and immunoblotted (WB:SYN1A) for SYN1A (HA IP-surf). Nonbound extracts were immunoprecipitated and blotted in parallel (HA IP-intra). Immunoblots of the total extracts (Total) show no impact of AMPH on SYN1A content. (D) The density of the immunoprecipitates bands (HA IP-surf and HA IP-intra) was normalized to the density of the

MOL #26690

correspondent parallel total extract and expressed as percentage of respective control. The normalized data are expressed as mean  $\pm$  SEM and compared to respective controls by Student *t*-test (\* = level of significance  $p < 0.001$ ;  $n=3$ ).

**Figure 6. KN93 blocks AMPH induced increase in hNET $\Delta_{28-47}$ /SYN1A associations.**

CAD cells, cotransfected both with HA-hNET $\Delta_{28-47}$  and SYN1A, were treated either with vehicle (CTR) or with 10  $\mu$ M KN93 for 30 min followed by 10  $\mu$ M AMPH for 1 min in the continuous presence of KN93 (KN93+AMPH). Surface proteins were labeled with NHS-sulfo-biotin at 4 °C before cell lysis and then recovered by using avidin beads. Bound hNET $\Delta_{28-47}$  proteins were immunoprecipitated with anti-HA antibody and resolved on SDS-PAGE, and immunoblotted for SYN1A (HA IP-surf). Nonbound extracts were immunoprecipitated and blotted in parallel (HA IP-intra). Immunoblots obtained from total extracts (Total) show that AMPH has no effect on SYN1A content. (B) The density of the immunoprecipitates bands (HA IP-surf and HA IP-intra) was normalized to the density of the correspondent parallel total extract and expressed as percentage of respective control. The normalized data are expressed as mean  $\pm$  SEM and compared to respective controls by Student *t*-test (\* = level of significance  $p < 0.01$ ;  $n=3$ ).

**FIG. 1**

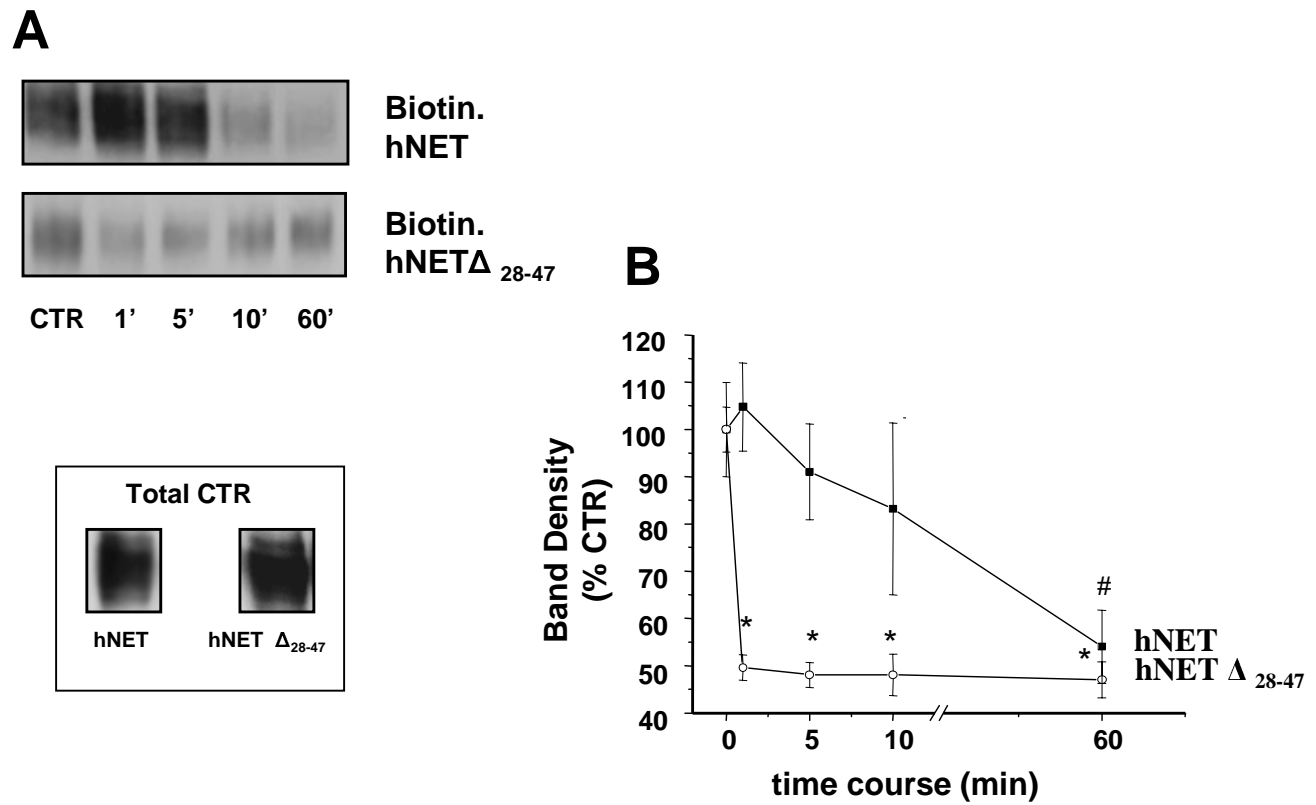
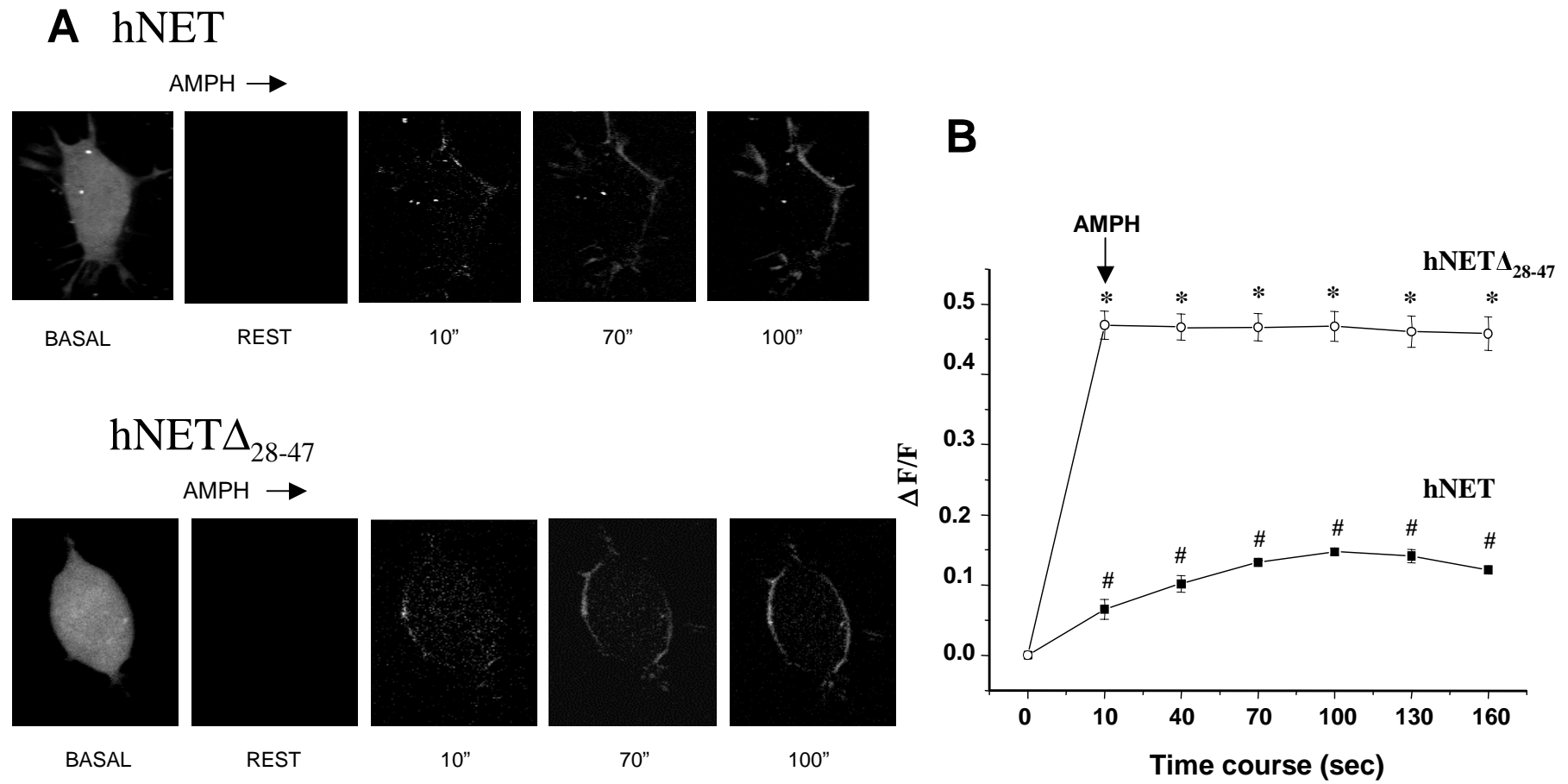
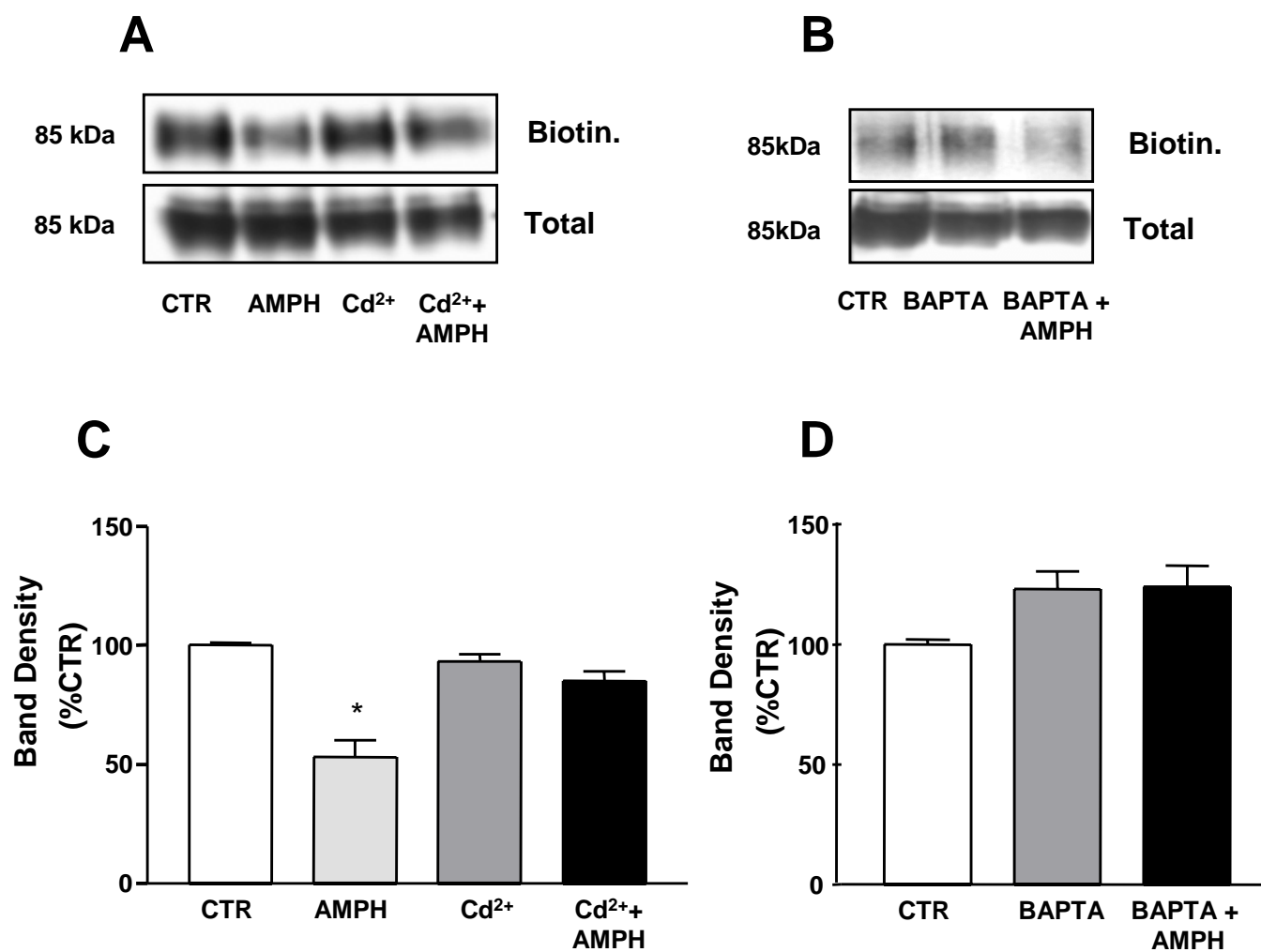


FIG. 2



**FIG. 3**

**hNET $\Delta_{28-47}$**



**FIG. 4**

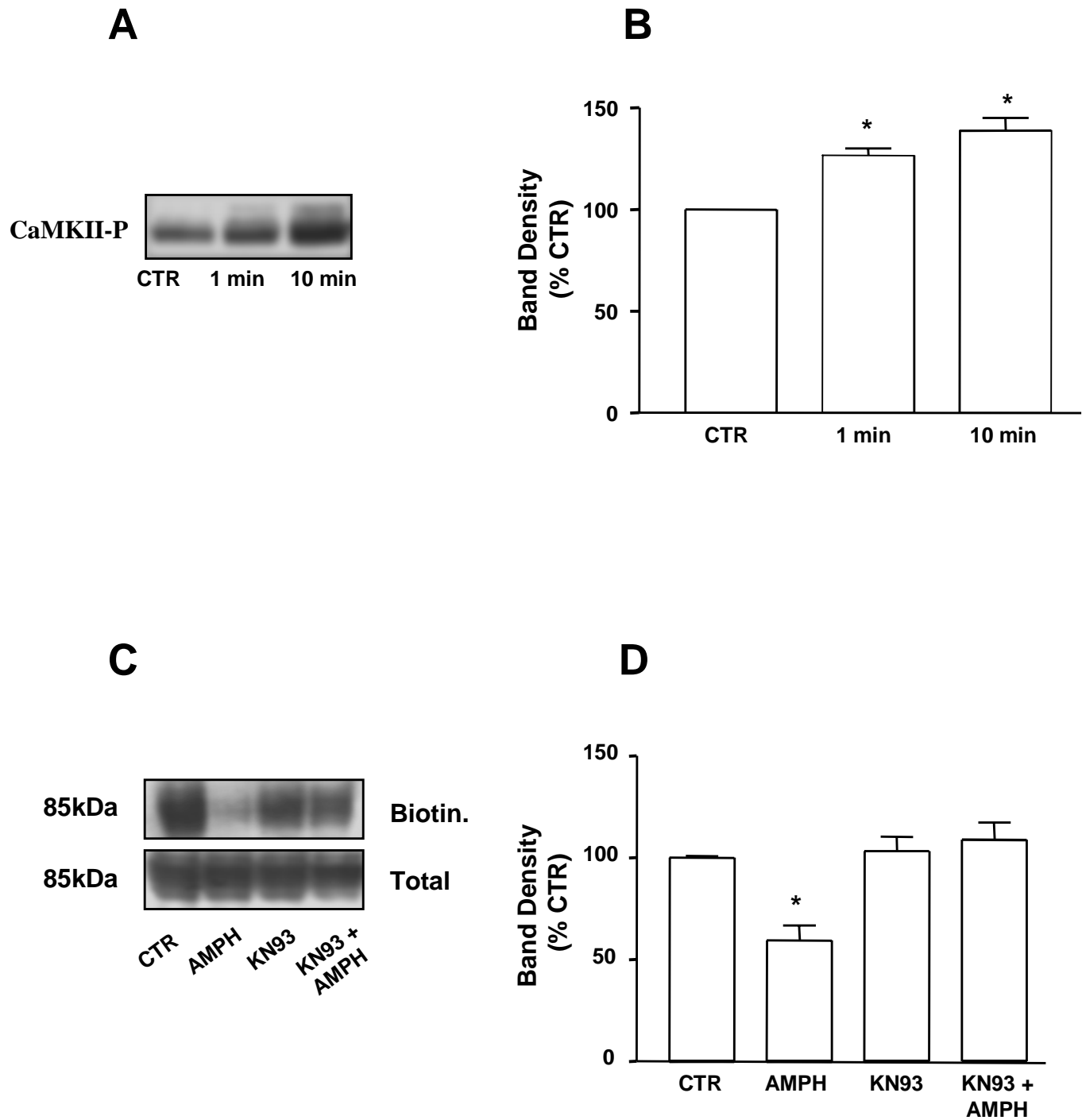
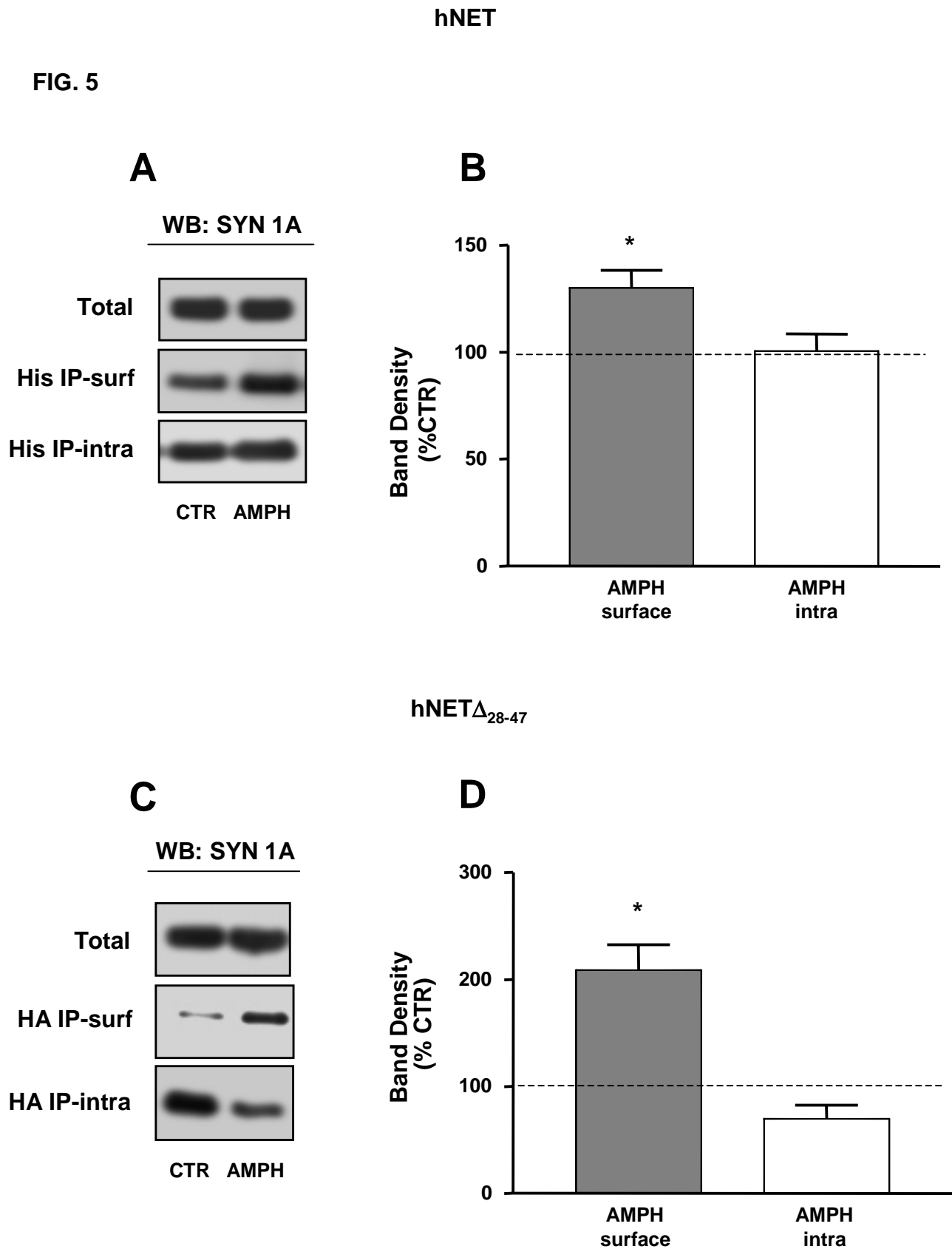




FIG. 5



**FIG. 6**

**hNET $\Delta_{28-47}$**

